

Additive Manufacturing of Multi-Material Parts Using PBF-LB—Enabling New Material Combinations

Constantin Jugert¹, Maja Lehmann¹, Georg Schlick¹, and Wolfram Volk²

¹ Fraunhofer Institute for Casting, Composite and Processing Technology IGCV,
Am Technologiezentrum 10, 86159 Augsburg, Germany

² Chair of Metal Forming and Casting (utg), TUM School of Engineering and Design, Technical
University of Munich, Walther-Meißner-Straße 4, 85748 Garching, Germany

Abstract

Producing complex parts from multiple materials using conventional technologies is challenging, time-consuming, and often uneconomical due to several manufacturing steps needed and increased costs. Multi-material powder bed fusion of metals using a laser beam (MM PBF-LB/M) enables new possibilities for processing several materials in a single manufacturing step and can significantly enhance functionality and lightweight potential, for example, in aerospace applications. However, defects in the transition zone of the materials, such as pores and cracks, pose an obstacle to further development and limit the use of MM PBF-LB/M. These defects often arise from mismatching energy inputs. By adjusting process-related parameters, the quality of the transition zone could already be improved. However, the experimental effort is high, and material-specific properties are often not considered. This paper presents an approach that takes material properties into account alongside process-related influences. A preliminary overview of these factors is provided. Furthermore, initial experiments were conducted for the combination of a copper alloy (CW106C) and a tool steel (1.2709), as well as for the combination of a ferromagnetic steel (1.4006) and a non-ferromagnetic steel (type750). By adjusting the scan vector distance, it was possible to create a bond with minimal defects. For the combination CW106C/1.2709, a distance of 80 μm resulted in a nearly defect-free connection. For 1.4006/type750, an overlap of 100 μm led to a qualitative bond, emphasizing the importance of material-specific factors. Therefore, understanding and influencing relevant factors, both material and process-related, is essential for standardized processing, which facilitates the production of innovative components.

Introduction

Powder bed fusion of metals using a laser beam has established itself as one of the most important additive manufacturing techniques and is used for many industrial applications [1]. In addition to rapid prototyping, series applications are increasingly found in the aerospace and automotive sectors [2]. In recent years, much research has been conducted into the further development of PBF-LB/M to produce novel multi-material parts [3]. The idea is that a component can be made not only from one material but from multiple materials, and in such cases, is referred to as a functionally graded material (FGM) [4, 5]. This is also possible with conventional manufacturing techniques such as casting or welding. However, MM PBF-LB/M can create added value precisely in this area, as the layer-by-layer build process and the use of a powder material feedstock allow for the local distribution of different materials. Due to the high complexity that can be achieved with PBF-LB/M, advantages over conventional manufacturing techniques arise. The distribution of different materials enables the creation of components with tailored properties

that best meet the requirements for a specific use case. An example of this is the production of an injection nozzle from the materials CW106C (CuCr1Zr) and 1.2709 (X3NiCoMoTi18-9-5) [6]. By combining the good thermal properties of the copper alloy and the high mechanical properties of the tool steel, the functionality of an industrially relevant component could be improved. A variety of materials and different machine concepts have been investigated in the past. However, a more general approach to manufacturing multi-material components using PBF-LB/M does not yet exist. This paper presents a concept that considers not only process-related factors but also material-specific properties. Relevant key factors are collected in a first step and classified into the categories material and process-related. Additionally, the influence of the scan vector distance on the quality of the transition zone for two industrially relevant material combinations is examined. This lays the foundation for the overall objective of finding and understanding relevant key factors, thereby enabling new material combinations for MM PBF-LB/M in the future.

State of the Art

Multi-material powder bed fusion of metals using a laser beam is the subject of current research and can be divided into the areas of in-situ alloying, two-dimensional (2D), and three-dimensional (3D) MM PBF-LB/M. In-situ alloying involves the mixing of different powder materials before or during the process. 2D MM PBF-LB/M includes those processes where conventional manufacturing techniques are combined with the standard mono-material process (hybrid) or where at least two mono-material processes are combined with material transitions in one direction. 3D MM PBF-LB/M finally refers to techniques that enable any spatial distribution of at least two materials in the component. All three areas will be presented below based on the state of the art.

In-situ alloying

Before the actual process, a powder mixture of several alloys can be produced and processed in the conventional PBF-LB/M process. This is referred to as in-situ alloying. The entry barrier is low, as conventional AM systems can be used without modification and possess a high technology readiness level (TRL). Theoretically, all powder materials that can be processed in the PBF-LB/M process can also be combined with each other. In the studies by WIMMER et al. [7], for example, 316L and AlSi10Mg were mixed in different fractions, processed, and examined using a novel setup. With the help of thermography and high-speed imaging, it was possible to quantify the melt pool depth during the process and compare it with the results of the metallographic analysis. By adding 20 mass-% AlSi10Mg to 316L, the variation in depth was reduced by 48%. This shows that, in addition to the influence of process parameters such as scan speed, as previously demonstrated in [8], the material composition and thus material-related factors also play a significant role for the process. The described form of MM PBF-LB/M can be extended so that the powder materials are mixed and applied layer by layer during the process itself, which allows for a targeted gradient of the chemical composition in the build direction. This was examined, for example, in [9] for the alloys Inconel 718 (IN718) and Ti6Al4V (Ti64). Up to a content of 10 mass-% IN718 in Ti64, the powder mixture was buildable but exhibited cracks—presumably due to the brittle intermetallic phase Ti_2Ni .

Two-dimensional (2D) MM PBF-LB/M

In addition to in-situ alloying, two-dimensional MM PBF-LB/M is frequently applied, as the entry barrier is also low and conventional PBF-LB/M systems can be used. The basic principle is to combine two different materials, where the first material is in the form of a build plate or a conventionally manufactured component and is complemented by the second material in the PBF-LB/M process, which is also referred to as hybrid PBF-LB/M [10]. A combination of several AM processes to produce multi-material components is also possible, such as PBF-LB/M and directed energy deposition of metals using a laser beam (DED-LB/M) [11, 12], DED-LB/M and DED-LB/M [13, 14], PBF-LB/M and laser foil printing (LFP) [15], and liquid dispersed metal powder bed fusion (LDM-PBF-LB/M) [16]. The material transition typically occurs in the build direction, which is why the term 2D MM PBF-LB/M has become established. The first layers or individual tracks on the build plate have been examined. CHEN et al. [17] discovered through in-situ X-ray monitoring that for the combination of a 316H substrate plate with IN718, a higher line energy density of up to 675 J/m resulted in a more diffuse interface. Melt pool depth, melt pool width, and mixing zone depth also increased, with a higher number of pores and cracks observed. NARAYANASWAMY et al. [18] continued these investigations and built 316L onto conventionally manufactured IN718. Additionally, a novel system concept was presented in [19], where Continuous Functionally Graded Materials (CFGMs) could be produced through separated areas in the powder reservoir. By adjusting the angle of the separating walls, different gradients could be achieved, which was investigated for 316L and a nickel-based superalloy.

In addition to using substrate plates or conventionally manufactured components as the second material, 2D MM PBF-LB/M can also represent the connection of two additively manufactured components from different materials. WANG et al. [20] combined layers of TiB₂ and Ti64 in a component and showed that residual stresses were particularly pronounced at the interface of the individual layers. The TiB nano-whiskers formed during the process positively affected the connection. SCHANZ et al. [21] developed a novel recoater that allowed for the combination of up to four different materials. This system can be used in conventional PBF-LB systems and for different lasers, providing high flexibility. To test the system, 316L was combined with the bronze CuSn10. Cracks that occurred in the structure could be attributed to three mechanisms: (i) significantly different melting points, (ii) different thermal expansion coefficients, and (iii) infiltration of bronze into the grain structure of 316L. The novel setup enabled different materials to be combined and examined, which is helpful for the development of new material combinations. Further investigations into the combination of 316L with CuSn10 can be found in [12, 17]. Unidirectional scan vectors in the transition zone without rotation in the surrounding layers positively affected the mechanical properties, which was attributed to improved grain growth in the transition area. WANG et al. [12] also found that for a build sequence of 316L → CuSn10, the best mechanical properties were achieved at an angle of 30° to the build plate—compared to 45°, 60°, and 90° to the build plate [22]. CORTIS et al. [23] investigated the processing of 316L with CuCr1Zr, noting that the poor absorption and high thermal conductivity of the copper alloy presented challenges, resulting in greater fluctuations in mechanical properties. This was also confirmed in [24], where similar experiments with this material combination were conducted and numerical simulations were performed. In particular, the mixing in the transition zone of the materials led to significantly altered optical properties and occasionally to a more pronounced reflectivity. Copper alloys are relevant in technical applications, as the high thermal conductivity of copper can be combined with the good processability of the copper alloy in the PBF-LB

process [5]. ZHANG et al. [25] processed IN718 and CuCr1Zr in a two-dimensional process and demonstrated strong diffusion of nickel into copper and vice versa. Further investigations into this material combination can be found in [26]. The size of the transition zone was about 750 μm in the experiments. Key factors influencing the mechanical properties included: (i) microcracks, (ii) element segregation, and (iii) microstructural inhomogeneities. CHEN et al. [27] focused on the combination of silver and copper. GUIMARÃES et al. [28] combined WC-Co and 316L. Other combinations in two-dimensional additive manufacturing of multi-material components include 316L with 15-5PH [29], 316L with AlSi10Mg [30], and 316L with 17-4PH [31]. The aim of most studies on two-dimensional additive manufacturing is to combine different materials and achieve a defect-free transition by influencing process parameters. However, certain combinations are difficult to join, as either thermophysical or metallurgical properties or both are too different. In such cases, it is often advisable to include one or more additional materials as transition layers. The aforementioned connection of IN718 and Ti64, for example, was improved in [32] by the use of niobium and copper interlayers, and in [33] by the use of a CuCr1Zr interlayer.

Three-dimensional (3D) MM PBF-LB/M

In the two-dimensional MM PBF-LB/M process, material transitions occur only in one spatial direction, usually the build direction. To fully utilize the advantages of different materials in a component, transitions in all three spatial directions need to be realized [34]. This means that in the layer-wise additive manufacturing process, material transitions must be possible not only between layers but also within a layer. Unlike 2D MM PBF-LB/M, this cannot be achieved with conventional PBF-LB systems, necessitating modifications to the equipment. According to SCHNECK et al. [35], there are fundamentally three concepts: (a) Holohedral, (b) Nozzle-based, and (c) Masked. All concepts are shown in Figure 1 and share the feature that they can process at least two different powder materials both within a layer and across layers.

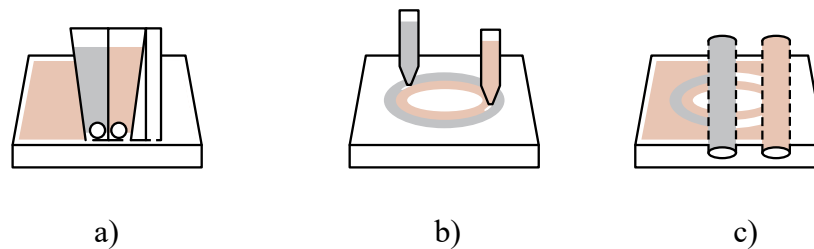


Figure 1: Comparison of the a) Holohedral, b) Nozzle-based, and c) Masked powder deposition concept adapted from [35]

An application for the nozzle-based technique can be found in [36]. With a modified system, it was possible to produce a battery cell cap made from two pure metals, aluminum and copper, as well as a ceramic mixture of 20 mass-% alumina and 80 mass-% zirconia (ATZ). This process also represents a challenging combination of 3D MM PBF-LB/M and the previously described in-situ alloying. Despite the very different thermophysical properties of the materials, a qualitative transition between them was achieved. A targeted calculation and consideration of shrinkage during pre-processing, as well as a stepwise transition between material areas, positively affected the connection.

The masked technique is also relevant and is often used due to higher powder coating rates. The basic principle is that the regions of the materials are already correctly captured by a mechanism, the mask, and deposited for a layer [35]. An example of the technique is the Selective Powder Deposition (SPD) system developed by Aerosint [37]. In this method, a drum is provided for each material, covered with a fine mesh. A vacuum allows the powder to be sucked to the surface of the drums and fixed at the voxel level. Specific material regions are then deposited on the build plate by rolling the drums and selectively opening valves at the bottom, enabling the processing of different powder materials within a layer [37]. MEYER et al. [38] provide helpful guidelines for processing 316L and CuCr1Zr with the SPD recoating technique. These investigations were expanded by DEILLON et al. [39], where defects like cracks in the 316L area and pores in the CuCr1Zr area were also observed. Besides adjusting process parameters, Hot Isostatic Pressing (HIP) was suggested to heal defects. Another methodology was developed where CuCr1Zr areas near the transition zone were not exposed to the laser but left in a powder state. Through subsequent HIP treatment, a very fine-grained structure with chromium-rich precipitates could be generated in these regions. Other material combinations investigated with the SPD coating technique include M300 (1.2709) with CuCr1Zr [37], 904L (1.4539) with bronze [40], and IN718 with Invar (64FeNi) [41]. The orientation of the transition zones significantly influences the quality of the material transition, according to [3] and [40]. For the three-dimensional MM PBF-LB/M process, it is crucial whether a material transition occurs within a layer (x-y) or across layers (z). Therefore, the orientation of the components in the build space plays an important role. The coating direction of the SPD recoater relative to the material transition within a layer had, according to GRIFFIS et al. [40], a comparatively minor influence on the quality of the joint zone. PRESTES AND JÄGLE [41] also noted that it is beneficial to process both materials within a layer using a continuous exposure strategy, which is only possible if the powder materials can be processed with identical parameters. This was the case for the combination of IN718 and Invar (64FeNi). However, the accuracy of powder deposition is limited when coating with a voxel-based mask. Current techniques can generate voxels with edge lengths down to a few hundred microns [35].

An alternative to the masked technique is the so-called holohedral powder coating, which derives its name from the Greek "holos" for "whole" and "hedra" for "face," meaning a "full-surface" coating. The resolution limit in this technique is only restricted by the laser and is therefore high [5]. The fundamental process involves fully coating with one material, then removing unsolidified powder after exposure and refilling the resulting cavities with another powder. This allows for three-dimensional material transitions to be created. Typically, suction is used to remove the powder material [35]. A system concept based on the principles of holohedral MM PBF-LB/M is presented in [42]. Notably, this system is capable of processing up to six different powder materials. The so-called Graded Alloy Processing (GAP) thus offers high flexibility in material selection. In experiments, titanium and tantalum, as well as IN718 and a copper alloy, were successfully processed together, with material transitions both within a layer and across layers. Another holohedral concept can be found in [43], where two spatially separated coaters and suction systems were used to manufacture test specimens from IN718 and pure copper. RINGEL et al. [44] used computer-aided topology optimization to manufacture a burner nozzle from IN718 and CuCrZr. A defined overlap of the scan vectors comparable to [45] had a positive effect on heat transfer but resulted in defects in the joining zone. RAVICHANDER et al. [46] illustrate an example of how a regular PBF-LB system can be modified to enable three-dimensional MM PBF-LB/M. In the experiments, the powder materials 316L and IN718 were successfully processed together with a customized SLM 125 PBF-LB machine. With a rotatable powder chamber containing two

reservoirs, it was possible in [47] to produce 3D multi-material components from the High Entropy Alloys (HEA) AlCuCoCrFeNi (AlCu-HEA) and MnCoCr (Mn-HEA). As discussed in the sections on in-situ alloying and 2D MM PBF-LB/M, the combination of IN718 and Ti64 was also investigated in the three-dimensional case. A key conclusion in [48] was that within a layer, the scan strategy significantly affects the thermomechanical behavior of the two materials near the transition zone. Scan vectors at an angle of 45° to the transition zone positively influenced energy distribution and prevented local overheating. This reduced residual stresses and defects. A material combination often studied in science and of technical relevance is CW106C (CuCr1Zr) and 1.2709 (X3NiCoMoTi18-9-5). The physical properties of the copper alloy, such as high thermal and electrical conductivity, along with the advantageous mechanical properties of the tool steel, make this combination interesting for many applications [49]. ANSTAETT [50] provides a guide for data preparation, selection of equipment technology, and recoating concepts using this material combination as an example. Building on this, SCHNECK et al. [6] manufactured an injection nozzle, achieving improved functionality through the combination of these two materials. Increased defect density was observed in the transition areas, manifesting as pores and cracks. Further investigations can be found in [51], focusing on the modification of a conventional PBF-LB system to produce three-dimensional multi-material components, supported by experiments combining CuCr1Zr and 1.2709. As the removal of the previously processed powder material within a layer is crucial for the holohedral recoating concept, studies were conducted by BARETH et al. [52]. Using simulation methods, a novel suction nozzle was designed and manufactured, allowing for significant improvement in suction homogeneity. This reduced cross-contamination in the components, which is essential for three-dimensional MM PBF-LB/M. The improved suction nozzle was used to produce another industrially relevant component, namely a radio-frequency quadrupole prototype [53]. A general approach for developing parameters for the transition zone of three-dimensional multi-material components is given by SCHROEDER et al. [5]. Guidelines demonstrating how to improve the quality of the transition zone using CuCr1Zr and 1.2709 as examples were provided. For a z-transition, a linear grading between the standard Volumetric Energy Densities (VEDs) of the two materials over several layers was proposed. The VED was calculated as

$$E = P/vht, \quad (1)$$

with the laser power P , scan speed v , hatch distance h and the layer thickness t . To enhance the material transition within a layer, remelting of the transition zone was investigated. Finally, a combination of both approaches with appropriate process parameters led to a reduction of defects in the transition zones and controllable properties of the transition area in the experiments.

Intermediate summary

- (i) The additive manufacturing of multi-material components can be accomplished using in-situ alloying, 2D, and 3D MM PBF-LB/M. The latter offers the possibility of providing material transitions both within a layer and across layers. This allows for a targeted adjustment of the material distribution in all three spatial directions, thereby achieving the highest functionality of the components.
- (ii) Material combinations that have been frequently investigated in the field of 3D MM PBF-LB/M include CW106C/1.2709, CW106C/316L, CW106C/IN718, IN718/316L, and IN718/Ti64. Defects such as pores and cracks in the transition zone are often analyzed, and strategies were developed to minimize them.

- (iii) Publications on 3D MM PBF-LB/M mainly focus on new machine concepts and the investigation of specific material combinations.
- (iv) There is a knowledge gap in the simultaneous consideration and investigation of process and material-related key factors. By connecting both areas, previously studied material combinations can be better understood, and new material combinations can be enabled for MM PBF-LB/M.

Concept

One of the biggest challenges in the field of 3D MM PBF-LB/M is the processing of different powder alloys with material transitions within a layer and in the build direction. The previous chapter has shown that numerous machine concepts with high technical maturity exist to produce three-dimensional multi-material parts, and selected material combinations have been processed together. However, the transition zones of the materials often exhibit numerous defects such as pores or cracks. To enable 3D MM PBF-LB/M for high-tech applications in the future, for example in the fields of aerospace and energy technology, the process must be further developed, and existing obstacles must be overcome. Some approaches exist, but they are often focused on a specific material combination, and the transferability to other materials is challenging. This paper presents a concept according to which key factors are crucial for a successful 3D MM PBF-LB/M process. The concept is schematically illustrated in Figure 2.

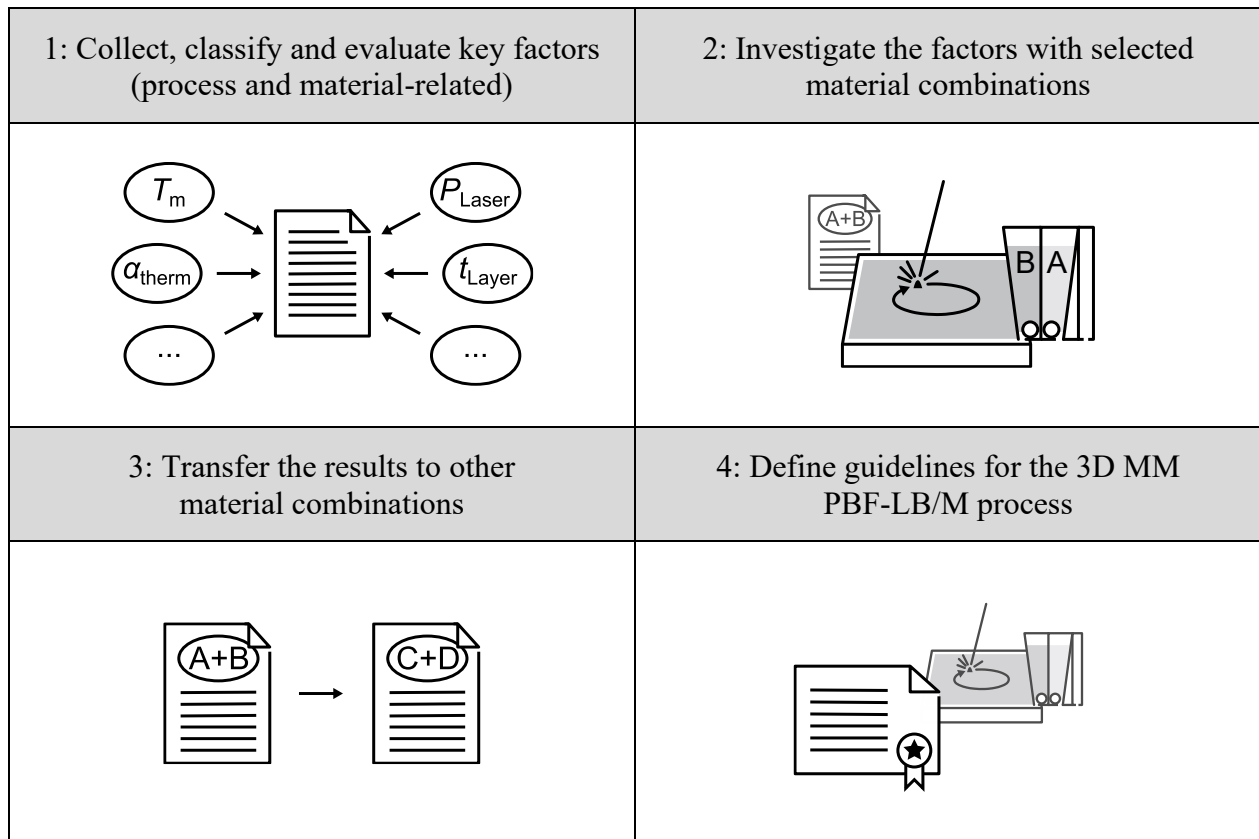


Figure 2: Concept to enable new material combinations

In the *first step*, key factors are collected, classified, and evaluated. The factors should be both process-related and material-related. In the *second step*, experiments are conducted to establish a connection between the theoretical factors and the real process. Here, the experience from previously conducted experiments can be utilized. The material combinations should be selected based on their suitability for investigating the factors and their technical relevance. In the *third step*, it will be examined how the findings can be transferred to other material combinations. The details of how this transfer can take place will then be developed. Finally, in the *fourth step*, guidelines should be provided regarding what needs to be considered for the investigated and future material combinations, as well as recommendations for the 3D MM PBF-LB/M process will be given. In a first approach, the key factors were divided into the areas of material-related factors and process-related factors. It should be noted that both areas—material and process—influence each other and are interdependent.

Material-related factors

The selection of two materials for the MM PBF-LB/M process often takes place based on the material properties that are critical for a specific application. For example, in the combination of CW106C and 1.2709, these are the good thermal conductivity of the copper alloy and the advantageous mechanical properties of the tool steel [5]. By defining the materials, the physical, mechanical, and metallographic characteristics are established. The properties of the powder materials are also defined. Important material-related factors can be found in Table 1.

Table 1: Material-related factors (excerpt)

Variable	Description	Unit
$T_m (T_l, T_s)$	Melting temperature (liquidus temperature, solidus temperature, phases)	°C
α_{therm}	Coefficient of thermal expansion	K ⁻¹
λ_{therm}	Thermal conductivity	W/m·K
$\rho_{\text{Material}}, \rho_{\text{Powder}}$	Density of the bulk material and powder	g/cm ³
$c_{\text{Material}}, c_{\text{Powder}}$	Specific heat capacity of the bulk material and powder	J/kg·K
τ_{Powder}	Powder flow behavior	s/50 g

Process-related factors

According to ANSTAETT [50], a selection of the system technology and coating technology must take place for the 3D MM PBF-LB/M process. These factors are inherent to the actual process. A corresponding selection could be, for example: holohedral powder coating system with suction mechanism. Furthermore, numerous factors can be influenced in the process. Important process-related factors are provided in Table 2.

Table 2: Process-related factors (excerpt)

Variable	Description	Unit
P_{Laser}	Laser power	W
v_{Laser}	Scan velocity	mm/s
h_{Distance}	Hatch distance	μm
t_{Layer}	Layer thickness	μm
E	Volumetric energy density	J/mm^3
d_{SVD}	Scan vector distance (between the material areas within a layer)	μm

One of the process-related factors that is investigated in this paper is the scan vector distance (d_{SVD}). As shown in Figure 3, it represents the distance between the scan vectors of the two material areas within a layer. It significantly influences the energy introduced by the laser near the transition zone, thereby affecting the bond. As different materials have varying melt pool sizes and shrinkage rates, it is necessary to adjust d_{SVD} to achieve a complete and uniform joint.

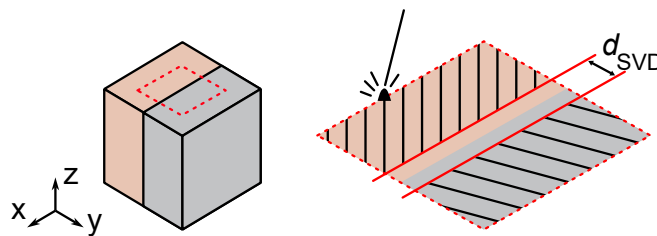


Figure 3: Schematic representation of the scan vector distance d_{SVD}

First results

Materials and Methods

First experiments that investigated the influence of the scan vector distance d_{SVD} were conducted for the material combinations CW106C/1.2709 and 1.4006/type750 (metals for printing *m4p*, Magdeburg, Germany). As previously explained in the state of the art, the combination of CW106C and 1.2709 is often used when both the thermal and electrical conductivity of the copper alloy and the mechanical properties of the tool steel are critical for a specific application [49, 50, 53]. The different magnetic properties of the martensitic chromium steel (1.4006) and the fully austenitic Ni-Cr-Mo steel (type750) are important in the second material combination. Both steels exhibit excellent weldability, good mechanical properties, and high corrosion resistance. A modified SLM 280^{HL} PBF-LB/M machine (Nikon SLM Solutions AG, Germany) was used for the investigations. The system was equipped with a divided holohedral powder recoating mechanism and a suction unit as described by SCHROEDER et al. [5]. For the experiments, a build chamber reduction was used with substrate plate dimensions of 100 mm · 100 mm. The build processes took place under a controlled argon atmosphere, and brushes were used for powder application. The process sequence for one layer could be divided into the steps (1.) coating with material A, (2.) solidifying of material A, (3.) removal of material A, (4.) coating with material B, (5.) solidifying of material B, and (6.) removal of material B. A schematic representation of the process steps is given in Figure 4. Steps (1.) to (6.) were repeated for each layer until the entire component was produced.

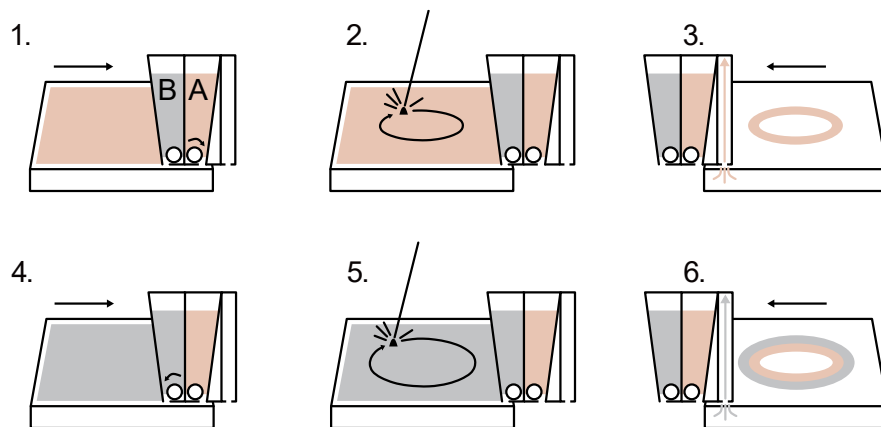


Figure 4: Schematic representation of the 3D MM PBF-LB/M process adapted from [5]

The properties of the powder materials used in the experiments can be found in Table 3.

Table 3: Chemical composition and Particle Size Distribution (PSD) percentiles of the powder materials used in the experiments

Material	Main alloying constituents in mass-%	PSD percentiles: $d_{10,3}/ d_{50,3}/ d_{90,3}$ in μm
CW106C	Cr (0.5), Zr (0.07), Cu (Balance)	16/ 28/ 44
1.2709	Ni (18), Co (8.8), Mo (4.9), Ti (1.1), Fe (Balance)	19/ 29/ 42
1.4006	Cr (12.1), Mn (0.8), Si (0.7), Fe (Balance)	21/ 32/ 45
type750	Ni (29.2), Cr (28.9), Mo (2.99), Mn (2.71), Fe (Balance)	21/ 31/ 42

In the MM PBF-LB/M process, the parameters given in Table 4 were used.

Table 4: Process parameters employed in the experiments

Material	P_{Laser} in W	v_{Laser} in mm/s	h_{Distance} in μm	t_{Layer} in μm	E in J/mm^3
CW106C	450	800	130	30	144.23
1.2709	200	800	120	30	69.44
1.4006	200	800	100	30	83.33
type750	200	800	100	30	83.33

In the experiments, a scan vector distance ranging from 180 μm to -70 μm in steps of 50 μm for the combination CW106C/1.2709 and a range of 0 μm to -500 μm in steps of 100 μm for the combination 1.4006/type750 was employed. In accordance with ANSTAETT [50], the exposure sequence for the first material combination was chosen so that within a layer, 1.2709 was exposed first, followed by CW106C. For the second material combination, type750 was exposed first, followed by 1.4006. The results are presented and discussed in the next section.

Results and Discussion

Figure 5 shows micrographs of the material combination CW106C/1.2709, where the cross-sectional images were taken in the x-y plane, thus parallel to the base plate and within a layer.

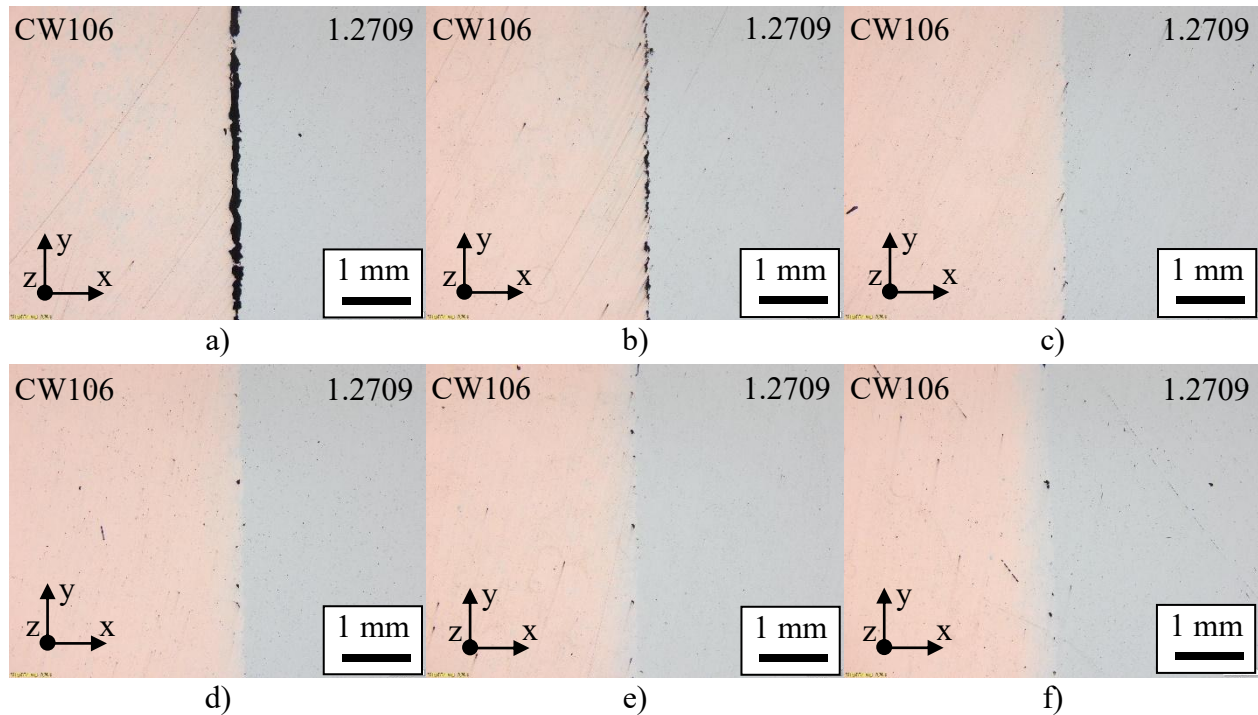


Figure 5: Micrographs of the combination CW106C/1.2709 with a d_{SVD} of a) $180 \mu\text{m}$, b) $130 \mu\text{m}$, c) $80 \mu\text{m}$, d) $30 \mu\text{m}$, e) $-20 \mu\text{m}$, and f) $-70 \mu\text{m}$

As can be seen, no complete connection between the material areas could be achieved for a scan vector distance of a) $180 \mu\text{m}$. This was expected, as the distance between the scan vectors prevented touching or even overlapping of the melt pools. With decreasing d_{SVD} , the distance between the CW106C and 1.2709 areas also decreased. At a value of c) $80 \mu\text{m}$, the gap between the material areas was closed, and a complete connection occurred for the first time. For all further values of d_{SVD} that were investigated, the connection remained intact.

Figure 6 shows microscopic images of the combination 1.4006/type750, where the cross-sectional images were made parallel to the z-axis, thus perpendicular to the base plate and in the build direction.

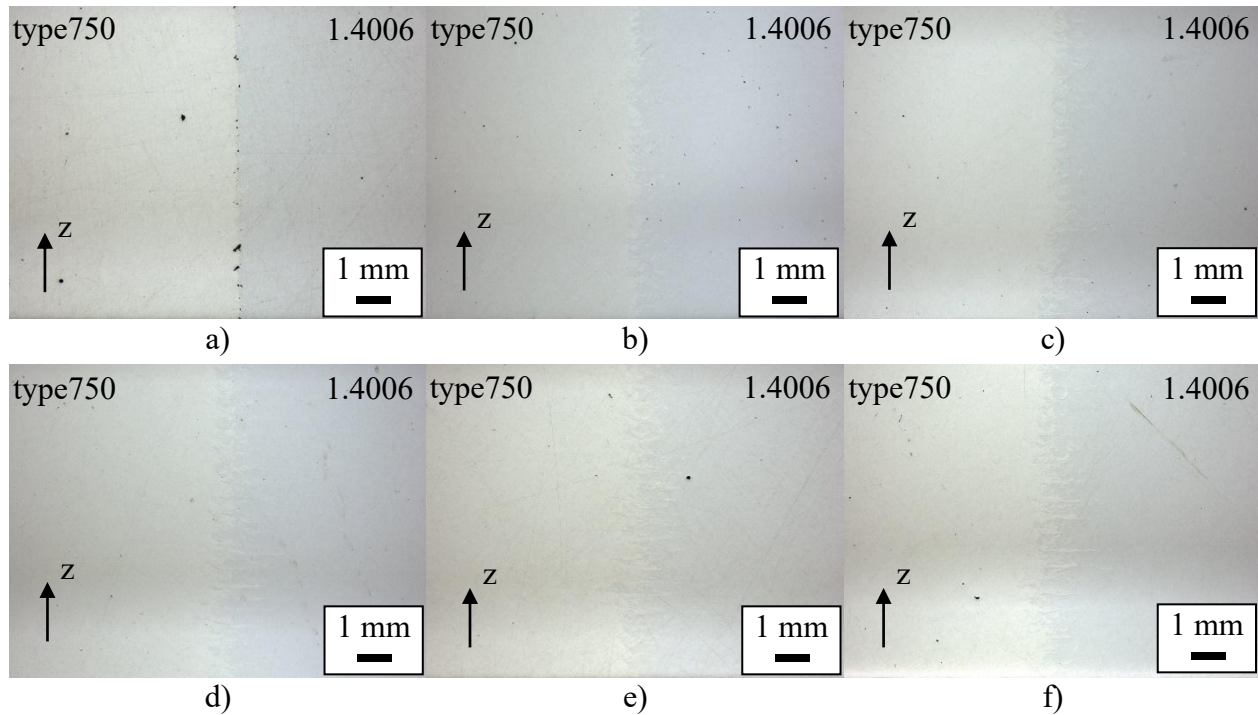


Figure 6: Micrographs of the combination 1.4006/type750 with a d_{SVD} of a) $0 \mu\text{m}$, b) $-100 \mu\text{m}$, c) $-200 \mu\text{m}$, d) $-300 \mu\text{m}$, e) $-400 \mu\text{m}$, and f) $-500 \mu\text{m}$

For the first chosen scan vector distance of a) $0 \mu\text{m}$, localized defects are visible. Just like in the combination CW106C/1.2709, the distance between the scan vectors of the two areas within a layer was too large to allow for a complete bonding of the materials. As d_{SVD} decreased, these defects along the interface disappeared, resulting in an almost defect-free transition zone. With decreasing values of d_{SVD} and thus increasing overlap, the intermixing of the two materials also increased, being largest in f) for a scan vector distance of $-500 \mu\text{m}$.

When comparing the influence of the scan vector distance d_{SVD} for both material combinations—CW106C/1.2709 and 1.4006/type750—the effects observed are similar. A too large scan vector distance resulted in no material-bonding contact being established, leaving a gap or lack of fusion defects along the joint. As d_{SVD} decreased, the distance between the solidified material areas also reduced, eventually leading to contact. This allowed for a connection with a low number of defects to be achieved in both cases. With increasing overlap, the mixing of the two materials increased. Accordingly, it was possible to influence and establish a qualitative bond between the materials for both combinations by adjusting the scan vector distance. Further investigations are needed to show how the different material-related properties, such as the coefficient of thermal expansion α_{therm} , have affected the bonding zone. In particular, the width of the melt pools and the shrinkage during cooling and solidification have a significant impact on the width of the gap between the two material areas. Therefore, d_{SVD} must be selected appropriately to ensure a uniform transition between the two materials that is as defect free as possible.

Conclusion and Outlook

In the present work, the PBF-LB/M process for the production of three-dimensional multi-material parts has been investigated. This form of the process, in which at least two different powder materials can be processed in any spatial distribution, has been studied in the past and may play a significant role in sectors such as aerospace, automotive, and energy in the future. Current research is particularly focused on the further development of machine technology and the investigation of specific material combinations, with a focus on process-related influencing factors. To further develop the process and overcome current obstacles such as pores and cracks in and near the transition zone, these process-related factors should be expanded to include material-related properties. The paper provides an initial overview of these key factors. Additionally, first experiments were conducted with the material combinations CW106C/1.2709 and 1.4006/type750. It was shown that a change in the scan vector distance has an impact on the characteristics of the transition zone for both material pairings. For the combination CW106C/1.2709, a distance of 80 μm led to a connection that was nearly defect-free. In the case of 1.4006/type750, a 100 μm overlap resulted in a high-quality bond. In the future, the relationship between the scan vector distance and relevant material-related properties, such as melting temperature and thermal expansion coefficient, will be investigated. This allows for the determination of optimal parameters for specified material properties. Ultimately, this will yield new insights that can be used to assess new material combinations.

The concept described in this paper needs to be further elaborated. An initial overview of important factors that need to be extended has already been provided. Furthermore, these factors need to be classified and evaluated according to their relevance. Methods will be found to investigate these factors based on selected material combinations. A first step in this direction has already been taken in the present paper. Additionally, it needs to be investigated how these findings can be transferred to other material combinations and whether there is a more general approach. Finally, guidelines for the MM PBF-LB/M process will be developed based on this.

Acknowledgements

We hereby express our gratitude to the European Union and its Horizon Europe program. Some of the illustrations and results in this paper were achieved within the scope of the research project “ENLIGHTEN-ED” (European Initiative for Low cost, Innovative & Green High Thrust Engine – Engine Demonstration) under grant agreement No 101135156.

References

- [1] Wohlers, T. T., Campbell, I., Diegel, O., Huff, R., and Kowen, J. (2022), Wohlers report 2022 : 3D printing and additive manufacturing global state of the industry / Terry Wohlers, Ian Campbell, Olaf Diegel, Ray Huff and Joseph Kowen. Fort Collins, Colorado: Wohlers Associates.
- [2] Shekh, M. J., Yeo, L. C., and Bair, J. L. (2024) “A review of 3D-printed bimetallic alloys,” *Int J Adv Manuf Technol*, vol. 132, 9-10, pp. 4191–4204, doi: 10.1007/s00170-024-13662-0.
- [3] Meyer, I., Messmann, C. O., Ehlers, T., and Lachmayer, R. (2025) “Additive manufacturing of multi-material parts – Effect of heat treatment on thermal, electrical, and mechanical part

- properties of 316L/CuCrZr,” *Materials & Design*, vol. 252, p. 113783, doi: 10.1016/j.matdes.2025.113783.
- [4] DIN EN ISO/ASTM TR 52912:2020-09: Additive manufacturing - Design - Functionally graded additive manufacturing, Beuth Verlag GmbH, Berlin.
- [5] Schroeder, T., Lehmann, M., Horn, M., Kindermann, P., Uensal, I., Michal, F., Lippus, A., Schlick, G., and Seidel, C. (2024) “Transition zone parameter development in multi-material powder bed fusion: a general approach,” *Prog Addit Manuf*, vol. 9, no. 3, pp. 613–624, doi: 10.1007/s40964-024-00663-4.
- [6] Schneck, M., Horn, M., Schindler, M., and Seidel, C. (2022) “Capability of Multi-Material Laser-Based Powder Bed Fusion—Development and Analysis of a Prototype Large Bore Engine Component,” *Metals*, vol. 12, no. 1, p. 44, doi: 10.3390/met12010044.
- [7] Wimmer, A., Hofstaetter, F., Jugert, C., Wudy, K., and Zaeh, M. F. (2022) “In situ alloying: investigation of the melt pool stability during powder bed fusion of metals using a laser beam in a novel experimental set-up,” *Prog Addit Manuf*, vol. 7, no. 2, pp. 351–359, doi: 10.1007/s40964-021-00233-y.
- [8] Wimmer, A., Lehmann, M., Schuler, A., and Zaeh, M. F. (2020) “Analysis of the phase transformation of AlSi10Mg during Laser Powder Bed Fusion,” *Procedia CIRP*, vol. 94, pp. 177–181, doi: 10.1016/j.procir.2020.09.034.
- [9] Scaramuccia, M. G., Demir, A. G., Caprio, L., Tassa, O., and Previtali, B. (2020) “Development of processing strategies for multigraded selective laser melting of Ti6Al4V and IN718,” *Powder Technology*, vol. 367, pp. 376–389, doi: 10.1016/j.powtec.2020.04.010.
- [10] ZainElabdeen, I. H., Ismail, L., Mohamed, O. F., Khan, K. A., and Schiffer, A. (2024) “Recent advancements in hybrid additive manufacturing of similar and dissimilar metals via laser powder bed fusion,” *Materials Science and Engineering: A*, vol. 909, p. 146833, doi: 10.1016/j.msea.2024.146833.
- [11] Bettencourt, C. J. and Kouraytem, N. (2023) “Microstructural Characterization of the Transition in SS316L and IN625 Bimetallic Fabricated Using Hybrid Additive Manufacturing,” *JOM*, vol. 75, no. 12, pp. 5079–5087, doi: 10.1007/s11837-023-06119-4.
- [12] Wang, X., Liu, Z., Tao, Y., Zhou, Y., Wen, S., and Shi, Y. (2023) “Enhancing the interface strength of additively manufactured 316 L/CuSn10 bimetallic components through heterogeneous microstructures,” *Additive Manufacturing*, vol. 78, p. 103860, doi: 10.1016/j.addma.2023.103860.
- [13] Sagong, M. J., Kim, E. S., Park, J. M., Karthik, G. M., Lee, B.-J., Cho, J.-W., Lee, C. S., Nakano, T., and Kim, H. S. (2022) “Interface characteristics and mechanical behavior of additively manufactured multi-material of stainless steel and Inconel,” *Materials Science and Engineering: A*, vol. 847, p. 143318, doi: 10.1016/j.msea.2022.143318.
- [14] Ghanavati, R., Naffakh-Moosavy, H., Moradi, M., and Eshraghi, M. (2022) “Printability and microstructure of directed energy deposited SS316L-IN718 multi-material: numerical modeling and experimental analysis,” *Scientific reports*, vol. 12, no. 1, p. 16600, doi: 10.1038/s41598-022-21077-8.
- [15] Rittinghaus, S.-K., Throm, F., Wilms, M. B., Hama-Saleh, R., and Rackel, M. W. (2022) “Laser Fusion of Powder and Foil – a Multi Material Approach to Additive Manufacturing,” *Lasers Manuf. Mater. Process.*, vol. 9, no. 4, pp. 569–589, doi: 10.1007/s40516-022-00190-6.
- [16] Bodner, S. C., Hlushko, K., van de Vorst, L., Meindlhumer, M., Todt, J., Nielsen, M. A., Hooijmans, J. W., Saurwalt, J. J., Mirzaei, S., and Keckes, J. (2022) “Graded Inconel-stainless steel multi-material structure by inter- and intralayer variation of metal alloys,”

- Journal of Materials Research and Technology*, vol. 21, pp. 4846–4859, doi: 10.1016/j.jmrt.2022.11.064.
- [17] Chen, W.-Y., Zhang, X., Li, M., Xu, R., Zhao, C., and Sun, T. (2020) “Laser powder bed fusion of Inconel 718 on 316 stainless steel,” *Additive Manufacturing*, vol. 36, p. 101500, doi: 10.1016/j.addma.2020.101500.
- [18] Narayanaswamy, S., Telasang, G., Park, N., and Bathe, R. (2025) “Additive manufacturing of SS316L-IN718 superalloy Bi-metallic structure: interfacial microstructure and mechanical properties,” *Prog Addit Manuf*, doi: 10.1007/s40964-025-01036-1.
- [19] Angelastro, A., Posa, P., Errico, V., and Campanelli, S. L. (2023) “A Systematic Study on Layer-Level Multi-Material Fabrication of Parts via Laser-Powder Bed Fusion Process,” *Metals*, vol. 13, no. 9, p. 1588, doi: 10.3390/met13091588.
- [20] Wang, R., Gu, D., Lin, K., Chen, C., Ge, Q., and Li, D. (2022) “Multi-material additive manufacturing of a bio-inspired layered ceramic/metal structure: Formation mechanisms and mechanical properties,” *International Journal of Machine Tools and Manufacture*, vol. 175, p. 103872, doi: 10.1016/j.ijmachtools.2022.103872.
- [21] Schanz, J., Islam, N., Kolb, D., Harrison, D. K., Silva, A. K. M. de, Goll, D., Schneider, G., and Riegel, H. (2022) “Individual process development of single and multi-material laser melting in novel modular laser powder bed fusion system,” *Prog Addit Manuf*, vol. 7, no. 3, pp. 481–493, doi: 10.1007/s40964-022-00276-9.
- [22] Chen, J., Zhang, M., Zhao, D., Bi, G., Bai, Y., Xiao, Y., and Di Wang (2024) “The impact of interfacial characteristics on the interfacial properties of 316 L/CuSn10 multi-material manufactured by laser powder bed fusion,” *Materials Characterization*, vol. 211, p. 113862, doi: 10.1016/j.matchar.2024.113862.
- [23] Cortis, D., Pilone, D., Grazi, F., Broggiato, G., Campana, F., Orlandi, D., Shinohara, T., and Planell, O. S. (2025) “Functionally graded material via L-PBF: characterisation of multi-material junction between steels (AISI 316L/16MnCr5), copper (CuCrZr) and aluminium alloys (Al-Sc/AlSi10Mg),” *Prog Addit Manuf*, vol. 10, no. 4, pp. 2455–2472, doi: 10.1007/s40964-024-00761-3.
- [24] Mao, S., Ren, Z., Liu, G., and Zhang, D. Z. (2024) “The effect of processing parameters on the molten pool dynamics during laser powder bed fusion of CuCrZr/316L multi-material,” *Journal of Materials Research and Technology*, vol. 31, pp. 1769–1785, doi: 10.1016/j.jmrt.2024.06.115.
- [25] Zhang, L., Dong, P., Zeng, Y., Yao, H., and Chen, J. (2024) “Additive manufacturing of Inconel 718/CuCrZr multi-metallic materials fabricated by laser powder bed fusion,” *Additive Manufacturing*, vol. 92, p. 104377, doi: 10.1016/j.addma.2024.104377.
- [26] Yang, X., Zou, G., Wang, Z., He, X., Zhang, M., and Xu, J. (2025) “Interfacial Characteristics and Mechanical Performance of IN718/CuSn10 Fabricated by Laser Powder Bed Fusion,” *Crystals*, vol. 15, no. 4, p. 344, doi: 10.3390/cryst15040344.
- [27] Chen, Q. et al. (2023) “High Reflectivity and Thermal Conductivity Ag-Cu Multi-Material Structures Fabricated via Laser Powder Bed Fusion: Formation Mechanisms, Interfacial Characteristics, and Molten Pool Behavior,” *Micromachines*, vol. 14, no. 2, doi: 10.3390/mi14020362.
- [28] Guimarães, B., Guedes, A., Fernandes, C. M., Figueiredo, D., Bartolomeu, F., Miranda, G., and Silva, F. S. (2023) “WC-Co/316L stainless steel joining by laser powder bed fusion for multi-material cutting tools manufacturing,” *International Journal of Refractory Metals and Hard Materials*, vol. 112, p. 106140, doi: 10.1016/j.ijrmhm.2023.106140.

- [29] Liang, A., Sahu, S., Zhao, X., Polcar, T., and Hamilton, A. R. (2023) “Interfacial characteristics of austenitic 316 L and martensitic 15–5PH stainless steels joined by laser powder bed fusion,” *Materials Characterization*, vol. 198, p. 112719, doi: 10.1016/j.matchar.2023.112719.
- [30] Miao, H., Yusof, F., Ab Karim, M. S., Wu, B., Raja, S., Ibrahim, M. Z., Aziz, I., and Chen, D. (2023) “Interfacial microstructure, element diffusion, mechanical properties and metallurgical bonding mechanism of 316L- AlSi10Mg multi-material parts fabricated by laser powder bed fusion,” *Journal of Materials Research and Technology*, vol. 26, pp. 8351–8365, doi: 10.1016/j.jmrt.2023.09.158.
- [31] McDonnell, B., Errico, V., Posa, P., Angelastro, A., Furman, A., O’Hara, E., Campanelli, S. L., and Harrison, N. (2024) “Bi-metallic lattice structures manufactured via an intralayer multi-material powder bed fusion method,” *Additive Manufacturing*, vol. 89, p. 104301, doi: 10.1016/j.addma.2024.104301.
- [32] Repnin, A., Borisov, E., and Popovich, A. (2024) “Formation of the Cu+Nb Interlayer in the Inconel 718/Ti6Al4V Multi-Material Obtained by Selective Laser Melting,” *Materials (Basel, Switzerland)*, vol. 17, no. 23, doi: 10.3390/ma17235801.
- [33] Wang, D., Li, Y., Liu, L., Tang, J., Yang, Y., and Han, C. (2025) “Interfacial Strain Behavior of Multi-material Structures Fabricated by Laser Powder Bed Fusion,” in *Mechanisms and Machine Science, Computational and Experimental Simulations in Engineering*, K. Zhou, Ed., Cham: Springer Nature Switzerland, pp. 460–472.
- [34] Kavousi Sisi, A., Ozherelkov, D., Chernyshikhin, S., Pelevin, I., Kharitonova, N., and Gromov, A. (2025) “Functionally graded multi-materials by laser powder bed fusion: a review on experimental studies,” *Prog Addit Manuf*, vol. 10, no. 4, pp. 1843–1912, doi: 10.1007/s40964-024-00739-1.
- [35] Schneck, M., Horn, M., Schmitt, M., Seidel, C., Schlick, G., and Reinhart, G. (2021) “Review on additive hybrid- and multi-material-manufacturing of metals by powder bed fusion: state of technology and development potential,” *Prog Addit Manuf*, vol. 6, no. 4, pp. 881–894, doi: 10.1007/s40964-021-00205-2.
- [36] Bareth, T., Eder, D., Lehmann, M., Schlick, G., and Seidel, C. (2025) “Multi-material additive manufacturing of conductor-insulator compounds for battery cell cap fabrication,” *Materials & Design*, vol. 254, p. 114010, doi: 10.1016/j.matdes.2025.114010.
- [37] Li, X., Sukhomlinov, D., and Que, Z. (2024) “Microstructure and thermal properties of dissimilar M300-CuCr1Zr alloys by multi-material laser-based powder bed fusion,” *Int J Miner Metall Mater*, vol. 31, no. 1, pp. 118–128, doi: 10.1007/s12613-023-2747-x.
- [38] Meyer, I., Oel, M., Ehlers, T., and Lachmayer, R. (2023) “Additive manufacturing of multi-material parts - Design guidelines for manufacturing of 316L/CuCrZr in laser powder bed fusion,” *Heliyon*, vol. 9, no. 8, e18301, doi: 10.1016/j.heliyon.2023.e18301.
- [39] Deillon, L., Abando Beldarrain, N., Li, X., and Bambach, M. (2024) “Coupling hot isostatic pressing and laser powder bed fusion: A new strategy to manufacture defect-free CuCrZr-316L steel multi-material structures,” *Materials & Design*, vol. 241, p. 112914, doi: 10.1016/j.matdes.2024.112914.
- [40] Griffis, J. C., Shahed, K., Meinert, K., Yilmaz, B., Lear, M., and Manogharan, G. (2025) “Multi-material laser powder bed fusion: effects of build orientation on defects, material structure and mechanical properties,” *npj Adv. Manuf.*, vol. 2, no. 1, doi: 10.1038/s44334-025-00020-5.

- [41] Prestes, I. B. and Jäggle, E. A. (2025) “Influence of the laser strategy on bi-metallic interfaces printed via multi-material laser-based powder bed fusion,” *Additive Manufacturing Letters*, vol. 13, p. 100274, doi: 10.1016/j.addlet.2025.100274.
- [42] Walker, J., Middendorf, J. R., Lesko, C. C., and Gockel, J. (2022) “Multi-material laser powder bed fusion additive manufacturing in 3-dimensions,” *Manufacturing Letters*, vol. 31, pp. 74–77, doi: 10.1016/j.mfglet.2021.07.011.
- [43] Marques, A., Cunha, Â., Gasik, M., Carvalho, O., Silva, F. S., and Bartolomeu, F. (2022) “Inconel 718–copper parts fabricated by 3D multi-material laser powder bed fusion: a novel technological and designing approach for rocket engine,” *Int J Adv Manuf Technol*, vol. 122, 3-4, pp. 2113–2123, doi: 10.1007/s00170-022-10011-x.
- [44] Ringel, B., Zaepfel, M., Herlan, F., Horn, M., Schmitt, M., and Seidel, C. (2022) “Advancing functional integration through multi-material additive manufacturing: Simulation and experimental validation of a burner nozzle,” *Materials Today: Proceedings*, vol. 70, pp. 296–303, doi: 10.1016/j.matpr.2022.09.241.
- [45] Anstaett, C., Seidel, C., and Reinhart, G. (2017) “Fabrication of 3D Multi-material Parts Using Laser-based Powder Bed Fusion,” *Solid Freeform Fabrication: Proceedings of the 28th Annual International*.
- [46] Ravichander, B. B., Jagdale, S. H., and Kumar, G. (2025) “Cost-effective and adaptable lab-scale multi-material system for LPBF,” *Int J Adv Manuf Technol*, vol. 137, 11-12, pp. 5585–5593, doi: 10.1007/s00170-025-15495-x.
- [47] Huang, G., Li, B., He, H., and Xuan, F. (2025) “Multi-material laser powder bed fusion additive manufacturing of architecturally designed dual-phase heterostructures using heterogeneous high-entropy alloys,” *Journal of Materials Processing Technology*, vol. 336, p. 118708, doi: 10.1016/j.jmatprotec.2024.118708.
- [48] Huang, Y., Wang, T., Liu, L., Li, Y., Han, C., Tan, H., Zhou, W., Yang, Y., and Di Wang (2025) “Thermomechanical Behavior and Experimental Study of Additive Manufactured Superalloy/Titanium Alloy Horizontal Multi-Material Structures,” *Metals*, vol. 15, no. 4, p. 454, doi: 10.3390/met15040454.
- [49] Horn, M., Langer, L., Schafnitzel, M., Dietrich, S., Schlick, G., Seidel, C., and Reinhart, G. (2020) “Influence of metal powder cross-contaminations on part quality in Laser Powder Bed Fusion: copper alloy particles in maraging steel feedstock,” *Procedia CIRP*, vol. 94, pp. 167–172, doi: 10.1016/j.procir.2020.09.032.
- [50] Anstaett, C. (2020) “Multimaterialverarbeitung mittels Laserstrahlschmelzen am Beispiel von metallischen Verbindungen mit der Kupferlegierung CW106C,” Dissertation, Lehrstuhl für Betriebswissenschaften und Montagetechnik, Technische Universität München, München.
- [51] Bareth, T., Binder, M., Kindermann, P., Stapff, V., Rieser, A., and Seidel, C. (2022) “Implementation of a multi-material mechanism in a laser-based powder bed fusion (PBF-LB) machine,” *Procedia CIRP*, vol. 107, pp. 558–563, doi: 10.1016/j.procir.2022.05.025.
- [52] Bareth, T., Fromm, N., Schroeder, T., Fuerstenau, J.-P., Horn, M., and Seidel, C. (2023) “Design and validation of a suction device to reduce cross-contamination in multi-material laser-based powder bed fusion,” *Procedia CIRP*, vol. 120, pp. 380–385, doi: 10.1016/j.procir.2023.09.006.
- [53] Brenner, S., Dickmann, M., Helm, R., Mitteneder, J., Schlick, G., Lehmann, M., Jugert, C., Nedeljkovic-Groha, V., Dollinger, G., and Mayerhofer, M. (2025) “A radio-frequency quadrupole prototype additively manufactured as a multi-material component,” *Prog Addit Manuf*, doi: 10.1007/s40964-025-01120-6.